PHYSICAL REVIEW E **86**, 045103(R) (2012)

# Predicted formation of localized superlattices in spatially distributed reaction-diffusion solutions

M. Tlidi,* G. Sonnino, and M. Bachir
*Faculté des Sciences, Université Libre de Bruxelles (U.L.B.), Service de Physique Mathématique, CP 231, Campus Plaine, B-1050 Bruxelles, Belgium*
(Received 2 March 2012; published 16 October 2012)

We study numerically the formation of localized superlattices in spatially distributed systems. We predict that in wide regions of the parameter space, stable localized, either bright or dark, superlattices may form in reaction-diffusion systems. Localized superlattices are patterns which consist of a piece of superlattice. Each single ring is surrounded by spots. The number of rings and their spatial distribution are determined by the initial conditions. The peak concentration remains unaltered for fixed values of the parameters.

DOI: 10.1103/PhysRevE.86.045103 PACS number(s): 82.40.Ck, 47.54.Fj, 82.40.Bj, 89.75.Fb

Localized structures belong to the class of dissipative structures found far from equilibrium [1]. The concept of dissipative structures was introduced, for the first time, in the context of reaction diffusion systems [2] and experimentally observed later [3]. Localized structures consist of stationary bright or dark spots which can be either independent or randomly distributed in space. They occur in various fields of nonlinear science, such as chemistry [4–6], plant ecology [7], and optics [8,9]. However, in all cases, despite the different physical origin, localized structures appear when the modulational or Turing instability is subcritical. This behavior is now well understood (see recent overviews on this issue [10,11]). Besides periodic and localized structures, many macroscopic nonequilibrium systems exhibit biperiodic superlattices or quasicrystal patterns. These structures are ordered in space and they occur through resonant interaction between unstable modes in spatially distributed systems [12,13]. Extended superlattices and quasicrystals have been theoretically predicted, and experimentally observed, in various spatially distributed systems such as two-frequency Faraday experiments [14], hydrodynamics [15], nonlinear optics [16], gas discharge systems [17], and reaction diffusion systems [18]. We address here the theoretical prediction of localized superlattices.

In this paper, we consider a simple reaction diffusion type of model: the FitzHugh-Nagumo system. As we shall see, this simple model may explain some relevant experimental observations. We show numerically that this model supports stable localized superlattices. They consist of a piece of superlattice state embedded in a homogeneous steady state (HSS). Their spatial distribution involves one or more stable rings surrounded by spots. The number of peaks and/or dips and their spatial distribution is determined by the initial conditions. The necessary conditions for obtaining the spatial localization are quite general. They are found in the subcritical domain involving two states: a HSS and an extended superlattice structure, which are both linearly stable.

The phenomenon of localized superlattices is robust and could be found in a wide area of science. Nature abounds with examples where the dynamics involves resonant interactions between unstable modes. The interaction between successive bifurcations having different wavelengths are common in many other fields of nonlinear science, such as laser physics and hydrodynamics. Our analysis could then be applied to other models, e.g., in optics [19], in other reaction diffusion systems [20]. In optics, localized structures, often called cavity solitons, attract growing interest due to their potential applications to the all-optical control of light, optical storage, and information processing [8,9].

Our treatment is based on the well-known FitzHugh-Nagumo system which was originally derived to describe nerve conduction and to capture the basic properties of excitable membranes [21], i.e.,

$$\partial_t u = f(u,v) + D_u \nabla^2 u, \quad \partial_t v = g(u,v) + D_v \nabla^2 v, \qquad (1)$$

where $f(u,v) = u - u^3 + \beta u v - v$ and $g(u,v) = \epsilon(\gamma u - v - a)$ with $\epsilon = T_u/T_v$ the ratio of characteristic chemical relaxation times of the activator $u$ and inhibitor $v$. Here $t$ is time and the Laplace operator $\nabla^2 = \partial_{xx} + \partial_{yy}$ acts in the $\mathbf{r} = (x,y)$ plane. The parameters $a$, $\gamma$, and $\beta$ control the relative position and the number of nullcline intersections. The diffusion coefficients are $D_u$ and $D_v$.

The homogeneous steady states $u_s$ and $v_s$ are solutions of $a = (-1 + \gamma + a\beta - \gamma\beta u_s + u_s^2)u_s$ and $v_s = \gamma u_s - a$. In what follows, we consider a regime where the HSSs are stable with respect to the steady bifurcation and focus on the regime of pattern-forming instabilities, namely, when the differential diffusion process $d = D_v/D_u > 1$.

Small amplitude deviations from the homogeneous steady states $u_s$ and $v_s$ are expressed in terms of Fourier modes $\exp(\omega_k t + i\mathbf{k}\cdot\mathbf{r})$, where $\mathbf{k}$ stands for the wave vector. The dispersion relation obeyed by the eigenvalues $\omega_k$ reads $\omega_k^2 - [1 - \epsilon - 3u_s^2 + \beta v_s - (1+d)k^2]\omega_k + \Delta = 0$, with $\Delta = -\epsilon(1 - \gamma + \beta\gamma u_s + \beta v_s - 3u_s^2) - [d(1 - 3u_s^2 + \beta v_s) - \epsilon]k^2 + dk^4 = 0$ with $k = |\mathbf{k}|$. Turing instabilities correspond to the occurrence of the zero real root ($\omega_k = 0$). Taking into account $v_s = \gamma u_s - a$, we solve the dispersion relation with $\omega_k = 0$ for $k^2$. The solutions of this equation are plotted as a function of $u_s$ in Fig. 1.

As a function of $k^2$, the eigenvalues curves $\omega_k$ pass through a maximum, i.e., $\partial_k \omega_k = 0$ at

$$k_{T\pm}^2 = \frac{\left(1 - a\beta + \beta\gamma u_{T\pm} - 3u_{T\pm}^2\right)d - \epsilon}{2d}, \qquad (2)$$

which corresponds to the fastest growing modes. The threshold $u_{T\pm}$ associated with these instabilities are the solution

*Fonds de la Recherche Scientifique F.R.S.-FNRS, Belgium.

 

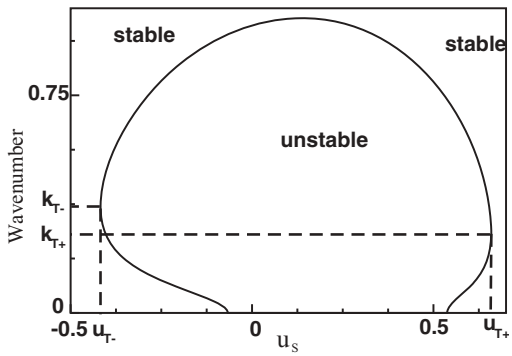


FIG. 1. Stability boundaries associated with two Turing instabilities for $d = 150$, $\beta = 0.7$, $\epsilon = 2.5$, and $\gamma = 0.9$. The wave number $k$ associated with the growing Fourier modes are shown in terms of the homogeneous steady states $u_s$.

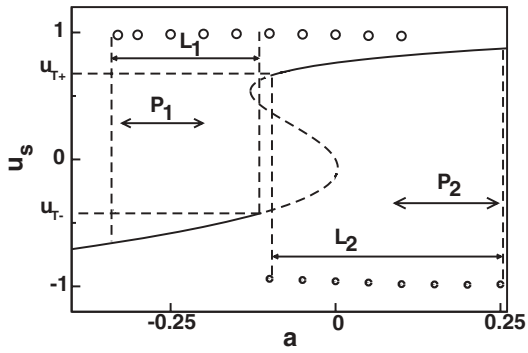


FIG. 2. Bifurcation diagram associated with extended superlattice patterns. The full and broken lines correspond, respectively, to stable and unstable homogeneous steady states. The white (black) circles indicate the maximum (minimum) of bright (dark) extended superlattice patterns. Parameters are the same as in Fig. 1.

of $[d(1-\beta a+\gamma\beta u_{T\pm}-3u_{T\pm}^2)-\epsilon]^2 = 4d\epsilon(\gamma-1+\beta a-2\beta\gamma u_{T\pm}+3u_{T\pm}^2)$. The system undergoes two Turing type of instabilities located at $u_{T+}$ and $u_{T-}$. The intrinsic wavelengths at both bifurcation points $\Lambda_{T-} = 2\pi/k_{T-}$ and $\Lambda_{T+} = 2\pi/k_{T+}$ are determined solely by the dynamical parameters and not by the boundary conditions or external constraints.

From Fig. 1, we see that as the homogeneous steady states $u_s$ increase, the succession stability-instability-stability occurs. First, all modes are damped when $u_s < u_{T-}$. Second, there appears a critical wave number $k_{T-}$ at $u_s = u_{T-}$, so that modes of wave number $k_{T-} < k < k_{T+}$ are amplified when $u_{T-} < u_s < u_{T+}$. In this range, the HSSs are unstable, i.e., $\omega_k > 0$ and there exists a band of unstable Fourier modes that triggers the spontaneous evolution of $u_s$ and $v_s$ towards a stationary spatially periodic or quasiperiodic distribution which occupies the whole space available in $(x,y)$ space. Third, there appears another critical wave number $k_{T+}$ at $u_s = u_{T+}$ such that all modes are again damped when $u_s > u_{T+}$. Indeed, in the first and the third cases, the eigenvalue $\omega_k < 0$, which ensures that fluctuations of finite wave number are damped and the HSS becomes then stable.

We first examine the formation of extended superlattice patterns corresponding to a superposition of the two unstable wavelengths $\Lambda_{T-}$ and $\Lambda_{T+}$. Due to the isotropy in $(x,y)$ space, these unstable modes have, *a priori*, no preferred direction. Although an indefinite number of modes may be generated with an arbitrary direction, a superlattice pattern is selected and emerges due to the nonlinear interactions. It has been shown that in the Fourier space, superlattice structures correspond to two resonant triplets: an equilateral triangle of length $|\mathbf{q_i}| = k_{T-}$ and three isosceles triangles of lengths $|\mathbf{Q_j}| = k_{T+}$ and $|\mathbf{q_i}| = k_{T-}$. These wave vectors should satisfy the following resonance conditions [12]: $\mathbf{q_1}+\mathbf{q_2}+\mathbf{q_3} = \mathbf{0}$, $\mathbf{q_1}+\mathbf{Q_1}+\mathbf{Q_2} = \mathbf{0}$, $\mathbf{q_2}+\mathbf{Q_3}+\mathbf{Q_4} = \mathbf{0}$, and $\mathbf{q_3}+\mathbf{Q_5}+\mathbf{Q_6} = \mathbf{0}$ with $|\mathbf{q_i}| = k_{T-}$ and $|\mathbf{Q_j}| = k_{T+}$. The angle $\phi$ between $\mathbf{Q_j}$ and $\mathbf{q_j}$ is $\phi = \arccos[k_{T-}/(2k_{T+})]$.

A direct numerical simulation of the model in Eqs. (1) on a square-shaped domain with periodic boundary conditions shows the occurrence of two types of extended superlattice patterns which can be either dark or bright. The results of this analysis are summarized in the bifurcation diagram of Fig. 2 where we plot the amplitude of the stationary solutions associated with both types of superlattice patterns versus the control parameter $a$. The spatial dynamics is very rich and complex. Besides the usual periodic structures such as hexagons, stripes, and rhombics, we focus on the formation of superlattice patterns. The initial condition used to generate these structures is

$$(u,v) = (u_s,v_s) + \mathbf{l_q}\sum_{i=1}^{3} m_i + \mathbf{l_Q}\sum_{j=1}^{6} M_i + \text{c.c.}, \qquad (3)$$

where $m_i = \bar{m}_i \exp(i\mathbf{q_j}\cdot\mathbf{r})$ and $M_i = \bar{M}_i \exp(i\mathbf{Q_j}\cdot\mathbf{r})$ with $\bar{m}_i$ and $\bar{M}_i$ the amplitude associated with the mode $k_{T-}$ and $k_{T+}$, respectively. $\mathbf{l_q}$ and $\mathbf{l_Q}$ are the eigenvectors of the linear operator at both bifurcation points. The c.c. denotes the complex conjugate. When increasing the control parameter $a$, the lower HSS is destabilized at the Turing instability $u_s = u_{T-}$, and a branch of bright superlattice pattern emerges as shown in the Fig. 2. By increasing further the control parameter, the upper branch of the HSS is stabilized at the second bifurcation (located at $u_s = u_{T+}$). From that bifurcation point, a branch of dark extended superlattice pattern emerges (see Fig. 2). As discussed above, these two types of phase-locked structures become stable due to the nonlinear interaction between two modes having different wave number and satisfying two resonant triplets. The two types of superlattice patterns have a wide overlapping domain of stability as shown in Fig. 2, and may coexist in the range of values of $a$ corresponding to the intersections of their stability domains.

In what follows, we focus our analysis on the formation of localized superlattices. Generally speaking, localized patterns consist of stationary bright or dark spots appearing on a HSS. Their existence requires a multistable regime, i.e., a coexistence of a HSS and a periodic structure such as hexagons and stripes [7–9,23]. However, when the system exhibits coexistence between stable HSS and extended superlattice patterns, stable localized superlattices may be generated. This is exactly what occurs in the domains $L_1$ and $L_2$ illustrated in Fig. 2. In these regimes, there exists a so-called pinning range of parameter values for which a stable localized superlattice, connecting the uniform and a branch of superlattice patterns, can be found. The pinning range associated with bright and dark localized superlattices $P_1$ and $P_2$, respectively, are shown

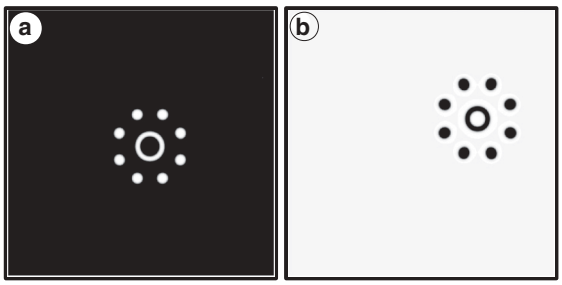


FIG. 3. (a) Bright and (b) dark localized superlattices corresponding to the activator $u$ obtained for $a = -0.25$ and for $a = 0.2$, respectively. Parameters are $d = 150, \beta = 0.7, \epsilon = 2.5$, and $\gamma = 0.9$. Maxima are plain white and the grid is $512 \times 512$.

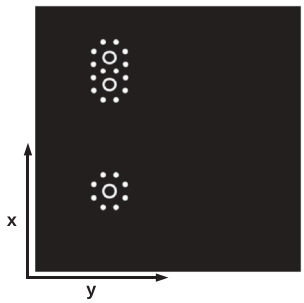


FIG. 4. Localized superlattices formed by three rings and spots corresponding to the activator $u$. Parameters are the same as in Fig. 3(a). Maxima are plain white and the grid is $800 \times 800$.

in Fig. 2. Examples of localized superlattices are shown in Fig. 3. To seed localized superlattices, we use an initial condition that consists of a slug of extended superlattice solution [Eq. (3)] embedded in a HSS with $m_i = 0.6$ and $M_i = 0.4$ for Fig. 3(a) and $m_i = -0.6$ and $M_i = -0.4$ for Fig. 3(b). Such a perturbation evolves towards stable localized superlattices. They are spatially localized in the sense that they are made by elements of extended superlattice patterns embedded in a uniform background. This localized superlattice possesses a well-defined size and it is stable with respect to parameter variations. Similar to extended superlattice patterns, localized superlattices can be either bright or dark as shown in Fig. 3. The simplest solution consists either of a bright or a dark ring surrounded by eight bright or dark spots (see Fig. 3). By removing the surrounding spots, the ring will be destabilized according to the well-known curvature instability [22]. Hence, the existence of stable spots ensures the stabilization of a ring.

Independent localized spots or rings can be formed at arbitrary positions in space. Their stability is independent of the spatial position. If, however, they are sufficiently close one to another, these structures start to interact due to the overlapping of their decaying oscillating tails. These spot-spot or spot-ring interactions will initiate a slow motion of localized rings or spots until when they reach a stable equilibrium position. The stabilization mechanism of rings is then attributed to the presence of spots that, through their interaction, allows the stabilization of localized superlattices. The remarkable feature of these solutions is that, depending on the initial conditions, we can generate an arbitrary number of stable localized rings and spots. Through the interaction, localized rings and spots gather themselves into a spatial configuration referred to as clusters. Stable clusters involving three-rings surrounded by spots, are shown in Fig. 4. These stationary localized states are aperiodic and consist of one or more regions in one state (homogeneous steady state) surrounded by a region in a qualitatively different state (extended superlattices). Neither of them grows in spite of available free $(x, y)$ space.

Localized structures offer short spatial range correlations in comparison to long-range correlations characteristic of extended patterns (periodic or biperiodic). Localized structures are often associated with storage of information in nonequilibrium systems [23]. However, extended patterns that can be either periodic or biperiodic, such as patterns, provide information only about wavelengths, and they are not suitable for storage or manipulation of information. This is due to the strong mutual correlation between spots and/or rings. By adding or removing a single spot or a single ring, the entire structure will be affected. Localized patterns are therefore more interesting for practical applications. Localized spots can be used as pixels for information storage and they may represent a two-state variable (i.e., "bits"). In our case, localized superlattices contain two types of localized objects: rings and spots, which differ in shape. This particular localized structure may represent a three-state variable. This increases the capacity of storage by a factor of $\log_2(3) \approx 1.58$.

Storage of information is an important issue in optical systems [8,9]. In particular, the semiconductor microcavity system has received special attention owing to its associated mature technology. The modeling of this system shows the occurrence of two subcritical Turing type of instabilities with different wavelengths [19] and its exhibits a variety of stable periodic and localized structures [9]. Dynamically speaking, apart from the phase of the electric field, this system and the FitzHugh-Nagumo model are similar. In particular, the marginal stability curve of the semiconductor microcavity (cf. to Fig. 5 of the paper by L. Spinelli *et al.* [19]) is similar to the one described in this paper (see Fig. 1). By varying the detuning parameter of this system we can easily satisfy the two resonant triplets describe above. Because this system satisfies the general conditions under which localized superlattices can be obtained, semiconductor microcavities are thus liable to produce some of the structures described in this paper.

We would like to point out that the nonvariational effect considered in this work is not an essential prerequisite for the stabilization of localized structures. Indeed, their stability in variational systems like the Swift-Hohenberg model indicates a functional monotonically decreasing in time. In this case, however, the formation of superlattices requires an interplay between two different unstable wavelengths generated by two coupled Swift-Hohenberg equations [13]. In this work the dynamics is governed by a free energy [13]. Hence, the existence of stable localized superlattices does not require nonvariational dynamics.

In conclusion, the numerical analysis of the FitzHugh-Nagumo equations allows us to identify stable localized superlattice patterns. These structures may be either bright or dark and involve isolated or self-organized spots and rings. This phenomenon occurs in the regime where the system exhibits a bistable behavior between a HSS and a branch of

an extended superlattice pattern. The mechanism lying at the basis of localized superlattices is the existence of two Turing instabilities having different wave numbers. This condition is rather general, and localized superlattice patterns could appear in a wide variety of systems far from equilibrium. In this respect, the stationary localized ring surrounded by spots has been observed experimentally in the Belousov-Zhabotinski reaction dispersed in a water-in-oil microemulsion [5], which is very similar to Fig. 3. This localized structure is attributed to the subcritical Turing instability and the formation of the ring may be induced by dust particles in the microemulsion. Here, we show that the origin of these localized structures is rather intrinsic. This means that the wavelengths, which determine the size of rings and spots, depend solely on the dynamical parameters and not on the boundary conditions or external forces or other external constrains. The formation of localized superlattices is rather induced by the subcritical extended superlattice branch of solutions.

G.S. is grateful to Dr. F. Zonca for his support. We thank Prof. R. Lefever for his scientific suggestions. This research is supported by the Interuniversity Attraction Poles program of the Belgian Science Policy Office, under Grant IAP P7-35 “photonics@be”.

[1] P. Glansdorff and I. Prigogine, *Thermodynamic Theory of Structures, Stability and Fluctuations* (Wiley, New York, 1971).

[2] A. M. Turing, Philos. Trans. R. Soc. London **237**, 37 (1952); I. Prigogine and R. Lefever, J. Chem. Phys. **48**, 1695 (1968).

[3] V. Castets *et al*., Phys. Rev. Lett. **64**, 2953 (1990); Q. Ouyang and H. L. Swinney, Nature **352**, 610 (1991).

[4] V. K. Vanag *et al*., Nature **406**, 389 (2000); I. Lengyel and I. R. Epstein, Proc. Natl. Sci. USA **89**, 128301 (2004).

[5] V. K. Vanag and I. R. Epstein, Phys. Rev. Lett. **92**, 128301 (2004).

[6] V. S. Zykov and K. Showalter, Phys. Rev. Lett. **94**, 068302 (2005).

[7] O. Lejeune *et al*., Phys. Rev. E **66**, 010901(R) (2002); E. Meron *et al*., Chaos Solitons Fractals **19**, 367 (2004); M. Rietkerk *et al*., Science **305**, 1926 (2004); E. Meron *et al*., Chaos **17**, 037109 (2007); M. Tlidi *et al*., Lect. Notes Phys. **751**, 381 (2008); E. Sheffer *et al*., J. Theor. Biol. **273**, 138 (2011).

[8] A. J. Scroggie *et al*., Chaos Solitons Fractals **4**, 1323 (1994); M. Tlidi *et al*., Phys. Rev. Lett. **73**, 640 (1994); **103**, 103904 (2009); A. G. Vladimirov, R. Lefever, and M. Tlidi, Phys. Rev. A **84**, 043848 (2011); F. Haudin *et al*., Phys. Rev. Lett. **107**, 264101 (2012).

[9] V. B. Taranenko *et al*., Phys. Rev. A **56**, 1582 (1997); Phys. Rev. Lett. **81**, 2236 (1998); S. Barland *et al*., Nature **419**, 699 (2002); X. Hachair *et al*., Phys. Rev. A **72**, 013815 (2005).

[10] V. S. Zykov, *Simulation of Wave Processes in Excitable Media* (Manchester University, Manchester, UK, 1987); J. D. Murray, *Mathematical Biology*, 3rd ed. (Springer, Berlin, 2003); A. S. Mikhailov and K. Showalter, Phys. Rep. **425**, 79 (2006); L. Pismen, *Vortices in Nonlinear Fields: From Liquid Crystals to Superfluids, From Nonequilibrium Patterns to Cosmic Strings* (Clarendon, Oxford, 1999); G. Purwins *et al*., Adv. Phys. **59**, 485 (2010).

[11] D. Mihalache *et al*., Prog. Opt. **27**, 229 (1989); K. Staliunas and V. J. Sanchez-Morcillo, *Transverse Patterns in Nonlinear Optical Resonators*, Springer Tracts in Modern Physics (Springer-Verlag, Berlin, 2003); Y. S. Kivshar and G. P. Agrawal, *Optical Solitons: From Fiber to Photonic Crystals* (Academic, New York, 2003); A. Malomed *et al*., J. Opt. B **7**, 53R (2005); M. Tlidi *et al*., Chaos **17**, 037101 (2007); N. Akhmediev and A. Ankiewicz, *Dissipative Solitons: From Optics to Biology and Medicine* (Springer-Verlag, Berlin, Heidelberg, 2008).

[12] S. Douady and S. Fauve, Europhys. Lett. **6**, 221 (1988); P. Coullet, T. Frisch, and G. Sonnino, Phys. Rev. E **49**, 2087 (1994); Z. H. Musslimani and L. M. Pismen, *ibid*. **62**, 389 (2000); G. Dewel *et al*., Faraday Discuss. **120**, 363 (2001); M. Bachir *et al*., Europhys. Lett. **54**, 612 (2001).

[13] T. Frisch and G. Sonnino, Phys. Rev. E **51**, 1169 (1995).

[14] A. Kudrolli *et al*., Phys. D **123**, 99 (1998); H. Arbell and J. Fineberg, Phys. Rev. E **65**, 036224 (2002).

[15] J. L. Rogers *et al*., Phys. Rev. Lett. **85**, 4281 (2000).

[16] E. Pampaloni *et al*., Phys. Rev. Lett. **78**, 1042 (1997); M. A. Vorontsov and B. A. Samson, Phys. Rev. A **57**, 3040 (1998); Y. A. Logvin *et al*., *ibid*. **55**, 4538 (1997).

[17] L. F. Dong *et al*., Phys. Rev. E **73**, 066206 (2006).

[18] I. Berenstein, L. Yang, A. M. Zhabontinsky, and I. R. Epstein, J. Phys. Chem. A **109**, 5382 (2005).

[19] L. Spinelli *et al*., Phys. Rev. A **58**, 2542 (1998).

[20] E. C. Odblom *et al*., J. Am. Chem. Soc. **108**, 2826 (1986); V. Gaspar and K. Showalter, *ibid*. **109**, 4869 (1987).

[21] R. FitzHugh, Biophys. J. **1**, 445 (1961); J. Nagumo *et al*., Proc. Inst. Radio. Eng. **50**, 2061 (1962).

[22] W. W. Mullins and R. F. Sekerka, J. Appl. Phys. **34**, 323 (1963); J. E. Pearson, Science **261**, 189 (1993); K. J. Lee *et al*., *ibid*. **261**, 192 (1993); R. Goldstein *et al*., Phys. Rev. E **53**, 3933 (1996); P. W. Davis *et al*., J. Phys. Chem. A **102**, 8236 (1998); C. B. Muratov and V. V. Osipov, Phys. Rev. E **53**, 3101 (1996); C. B. Muratov, *ibid*. **66**, 066108 (2002); Y. Hayase and T. Ohta, Phys. Rev. Lett. **81**, 1726 (1998); Phys. Rev. E **62**, 5998 (2000); M. Tlidi *et al*., Phys. Rev. Lett. **89**, 233901 (2002); T. Kolokolnikov and M. Tlidi, *ibid*. **98**, 188303 (2007); J. M. Soto-Crespo *et al*., Opt. Express **16**, 15388 (2008).

[23] P. Coullet *et al*., Phys. Rev. Lett. **84**, 3069 (2000); P. Coullet, C. Toniolo, and C. Tresser, Chaos **14**, 839 (2004).